

# **ANALYTICAL PERFORMANCE STUDY OF SUCTION PILES IN CLAY**

by

S. Bang<sup>1</sup> and Y. Cho<sup>2</sup>

## **ABSTRACT**

Using a three dimensional finite element method of analysis, an analytical feasibility study on suction piles in clay was conducted. Elasto-perfectly plastic soil properties were used to evaluate the effect of various cross-sectional shapes on the overall performance. Results of soil stresses and pile displacements under vertical, horizontal, and inclined loads were evaluated and compared.

## **INTRODUCTION**

The US Navy is currently conducting a technical feasibility study pertaining to the construction of Mobile Offshore Bases (MOBs). This is expected to be a self-propelled, floating military base with a runway on top and other supporting facilities below such as living quarters, material storage areas, docking facilities for transport ships, etc. The proposed dimensions of the MOB are approximately 5,000 feet by 500 feet. It is intended to be a forward-deployed, self-contained military base floating in deep waters. The South Dakota School of Mines and Technology is participating in this MOB feasibility study to provide an adequate mooring technique for this very large floating structure. The MOBs are expected to be controlled by dynamic positioning. However, during storage, repair, or lay-up periods, or for hybrid mooring, conventional mooring techniques may be needed. Suction piles are currently being investigated analytically and experimentally to provide the necessary mooring capability.

Suction piles typically have a large diameter (up to 100 feet to date) with a relatively small length-to-diameter ratio. They are installed by applying a suction pressure inside the pile, which acts as an external surcharge to push the pile into the seafloor. They may be retrieved later by applying a positive pressure inside the pile.

This paper describes the results of an analytical performance study on suction piles embedded in a clayey seafloor, using a three-dimensional finite element method of analysis. Three cross-sectional shapes that were thought to be able to provide adequate bearing resistance against various external loads were selected. They include circular, Y-

---

1, 2: Department of Civil and Environmental Engineering, South Dakota School of Mines and Technology, Rapid City, SD 57701

shaped, and triangular cross-sections. These suction pile cross-sections were analyzed using the extended Drucker-Prager plasticity constitutive model to represent the complex behavior of the clayey seafloor soil for detailed comparisons of their relative responses. Results of the plastic analysis, including the pile displacements and soil stresses, were compared in detail to identify the effectiveness of various suction pile cross-sections. The results of this study have been used in planning the laboratory model tests on suction piles.

## **DESCRIPTION OF ANALYSIS**

ABAQUS version 5.7 (1997), a comprehensive three-dimensional finite element method of analysis software written by Hibbit, Karlsson & Sorensen, Inc. was utilized for the finite element analysis. Additionally, FEAMAP software (1986 - 1996), written by Enterprise Software Products, Inc., was used for the easy performance of pre- and post-processing of input and output such as three-dimensional mesh generation, graphical output, etc.

### **Model Development**

The detailed dimensions of the selected piles were determined based on the same soil-pile contact area to keep the amount of the pile material the same. In addition, the length of the pile was chosen as 30 feet, and a cylindrical pile with 30 feet in diameter was selected as the control. The selected cross-sections were extended into three-dimensional columns to simulate the suction piles of constant cross-sections. The cylindrical outer surface of the pile was modeled by shell elements.

### **Material Properties**

It was assumed that the soil was homogeneous and isotropic. The behavior of the sand was characterized with elasto-perfectly plastic material properties. The initial elastic behavior of the clayey soil was described by Young's modulus ( $E$ ) and Poisson's ratio ( $\nu$ ), whereas the subsequent plastic behavior was modeled by the extended Drucker-Prager plasticity model (Drucker and Prager, 1952). In the extended Drucker-Prager plasticity model, yielding of the material is described differently in tension and compression. In general, relatively smaller resistance against tension than compression is allowed, i.e., the kinematic hardening plastic behavior. In addition, the maximum tensile yield stress (tension cut-off) of the soil was prescribed in the hyperbolic extended Drucker-Prager plasticity model.

The hyperbolic extended Drucker-Prager plasticity model was utilized to simulate the plastic behaviors of the clay under relatively larger loads. The hyperbolic Drucker-Prager model is a continuous combination of the maximum Rankine tensile stress condition (tension cut-off) and the linear Drucker-Prager condition at high confining stresses. The tension cut-off defined in the hyperbolic extended Drucker-Prager model is intended to reduce any potential error associated with the tension in the analysis with linear constitutive models. The hyperbolic model utilizes a linear assumption at high

confining pressures but it provides a nonlinear relationship between the deviatoric and mean confining stress at low confining pressures. The hyperbolic flow potential function approaches the linear Drucker-Prager flow potential asymptotically at high confining pressures and intersects the hydrostatic pressure axis ( $p$ ) at 90 degrees. Typical soil parameters, such as the soil friction angle and cohesion, can be converted to equivalent Drucker-Prager parameters. The following shows how the linear extended Drucker-Prager model (or hyperbolic extended Drucker-Prager model at high confining pressures) parameters for soils with low friction angles are obtained to duplicate the same failure definition as in triaxial compression and tension.

$$\begin{aligned} \text{Slope Angle } (\beta) &= \tan^{-1} \left( \frac{6 \sin \mathbf{f}}{3 - \sin \mathbf{f}} \right) \\ \text{Initial compressive yield stress } (\sigma_{\text{clo}}) &= \frac{2C \cos \mathbf{f}}{1 - \sin \mathbf{f}} \end{aligned}$$

The following clayey seafloor soil properties were quoted from Taylor (1982) and evaluated with the information from ABAQUS (1997) and Lade (1976).

Soil Classification = Organic Silty Clay of High Plasticity

Water Content (w) = 110 -160 %

Liquid Limit (LL) = 117 -142

Liquidity Index (LI) = 0.88 - 1.65

Total Soil Unit Weight ( $\gamma_t$ ) = 86 pcf

Sea-water Unit Weight ( $\gamma_w$ ) = 64 pcf

Buoyant Soil Unit Weight ( $\gamma_b$ ) = 22 pcf

Initial Void Ratio ( $e_o$ ) = 3.7

Cohesion (C) = 150 psf

Friction Angle ( $\phi$ ) = 5.0 deg (corresponding to slope angle of 10.2 deg in hyperbolic extended Drucker-Prager model)

Lateral Earth Pressure Coefficient ( $K_o$ ) = 0.91

AISI 4340 steel was chosen for the pile material. The pile was modeled by linear elastic properties, i.e., Young's modulus (E) of  $29 \times 10^6$  psi and Poisson's ratio ( $\nu$ ) of 0.32. In the analysis, however, the pile stiffness was assumed to be very large so that the pile deformations did not affect the soil deformations.

## Cross-sectional Shapes

The three cross-sectional shapes studied include circle, Y-shape, and triangle. The triangular section had three equal sides. The Y-shaped cross-section had three branches spaced at 120 degrees apart with identically shaped branches. Each branch consisted of a square, i.e., the width and height were the same.

## **RESULTS OF ELASTO-PLASTIC ANALYSIS**

The main objective of this study is to identify the most efficient suction pile cross-sectional shape through quantitative comparisons of the responses of the selected suction pile cross-sections with elasto-perfectly plastic soil properties under different loading conditions. The loads were applied along the horizontal direction, vertical direction, and direction inclined at 45 degrees to the horizontal. All loads were applied at the center of the pile cap. Vertical and inclined loads were applied away from the suction piles to create tension.

To simulate the in-situ field conditions, the geostatic state satisfying the prescribed boundary conditions was established before the external loads were applied. The gravity load, due to the soil buoyant unit weight, was applied as a distributed body force. Loads and prescribed initial stresses should be in exact equilibrium and produce zero deformations under the geostatic stress condition.

The load was increased incrementally and the behavior of the suction pile was observed in detail at various load levels for the different loading directions until the solutions, such as displacements and soil stresses, approached the ultimate values.

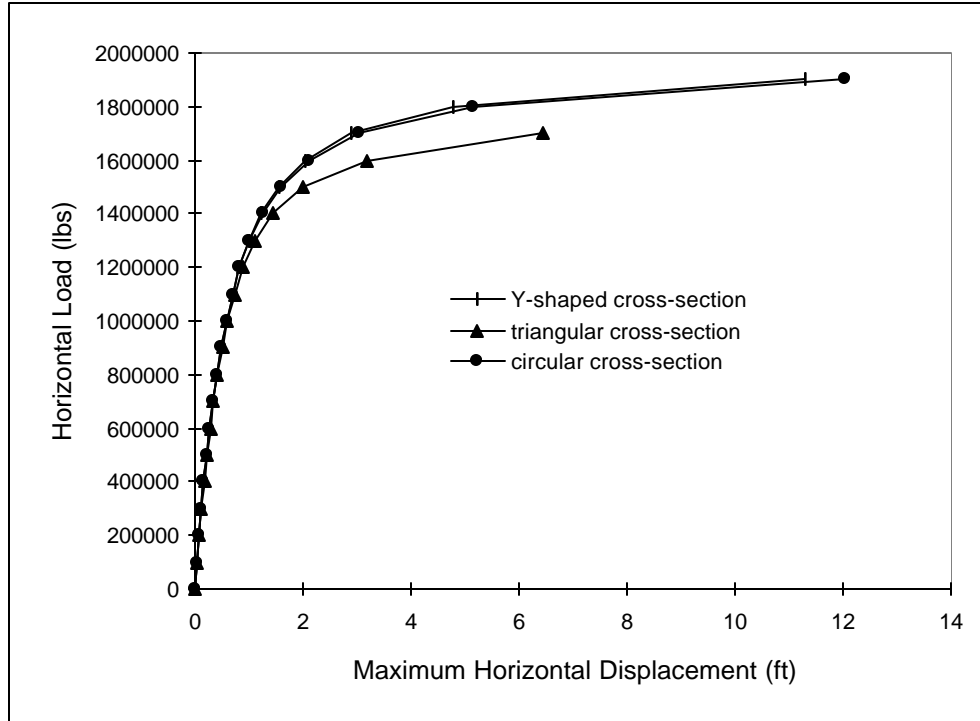
### **Behaviors of Suction Piles under Horizontal Loads**

#### **1) Pile Displacements**

Figure 1 shows the variations of the maximum horizontal pile displacements under various horizontal loads with different pile cross-sections. The maximum horizontal pile displacement represents the maximum pile displacement at any point within the pile along the loading direction. The maximum horizontal pile displacement always occurred at the top of the pile along the loading direction, whereas the minimum pile displacement occurred at the bottom of the pile. The pile was experiencing horizontal translational movements as well as rotational movements (Bang and Cho, 1998).

As can be seen from the figure, the displacements varied linearly due to the elastic behavior under relatively small loads. As the load increased, the displacements showed a nonlinear behavior due to the inclusion of the plastic soil behavior. The variations of the curves are more or less hyperbolic shaped and, hence, it is expected that the horizontal loads will eventually approach the ultimate values. The ultimate horizontal loads were observed approximately to be 2,000,000 lbs for the circular and Y-shaped cross-sections, and 1,800,000 lbs for the triangular cross-section. Almost identical displacements under various horizontal loads were observed with the circular and Y-shaped cross-sections when the loads were less than 1,600,000 lbs. Generally, the circular cross-section generated the smallest maximum horizontal displacements under the loads of up to 1,100,000 lbs. Beyond this load, the Y-shaped cross-section yielded the smallest displacements. The triangular cross-section generated the largest displacements for the entire range of the applied horizontal loads. The effect of the cross-sectional shape became very pronounced at relatively larger horizontal loads near the failure.

Figure 1. Maximum Horizontal Pile Displacement vs. Horizontal Load



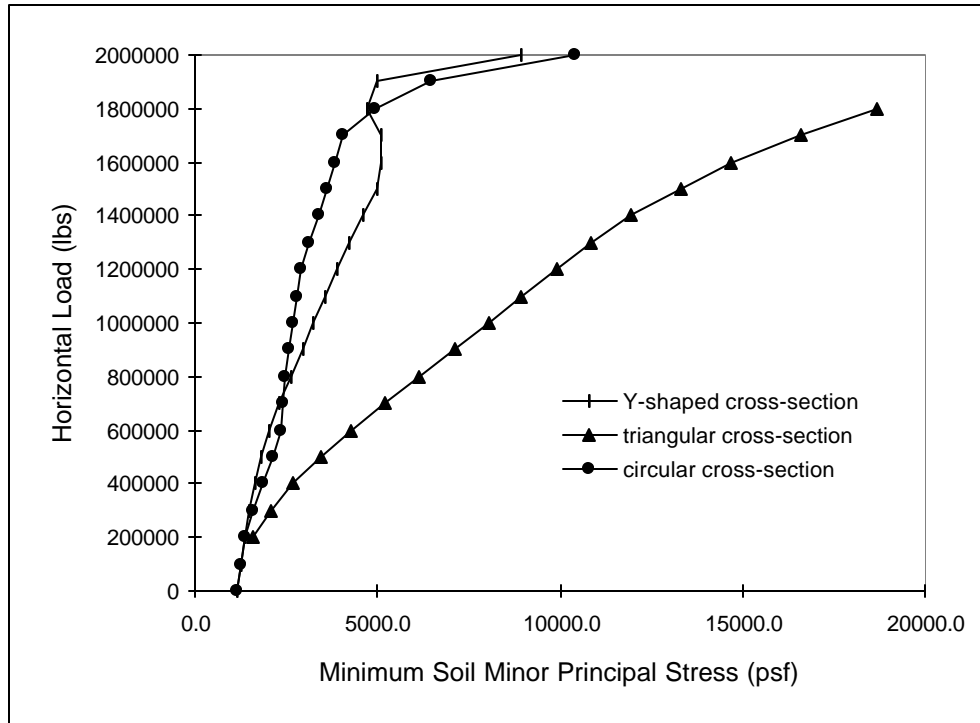
## 2) Minimum Soil Minor Principal Stresses

The minimum soil minor principal stress describes the absolute maximum soil compressive stress. Yielding of the soil starts within the highly stressed element when the largest principal stress within that element reaches the yield stress (Ugural and Fenster, 1995).

The minimum soil minor principal stress at any given horizontal load was always generated near the bottom of the advancing side of the pile. On the other hand, the receding side of the pile experienced relatively small tensile stresses due to the nature of kinematic hardening in the plastic analysis (Bang and Cho, 1998).

Figure 2 shows the relationships between the minimum soil minor principal stress and the applied horizontal load. The most effective cross-section in terms of the minimum soil minor principal stress depended on the applied load level. Almost identical minimum soil minor principal stresses for all cross-sections were observed under the horizontal load of 100,000 lbs, mainly because the developed stresses were not large enough to overcome the geostatic stresses. Once the geostatic stresses were overcome, the minimum soil minor principal stresses increased following various patterns. As can be seen from the figure, the patterns are not consistent. The seemingly irregular variations of the stresses may occur for many reasons, including 1) numerical errors due to the relatively large displacements within each load increment, and 2) difference in locations of elements where the minimum soil minor principal stresses

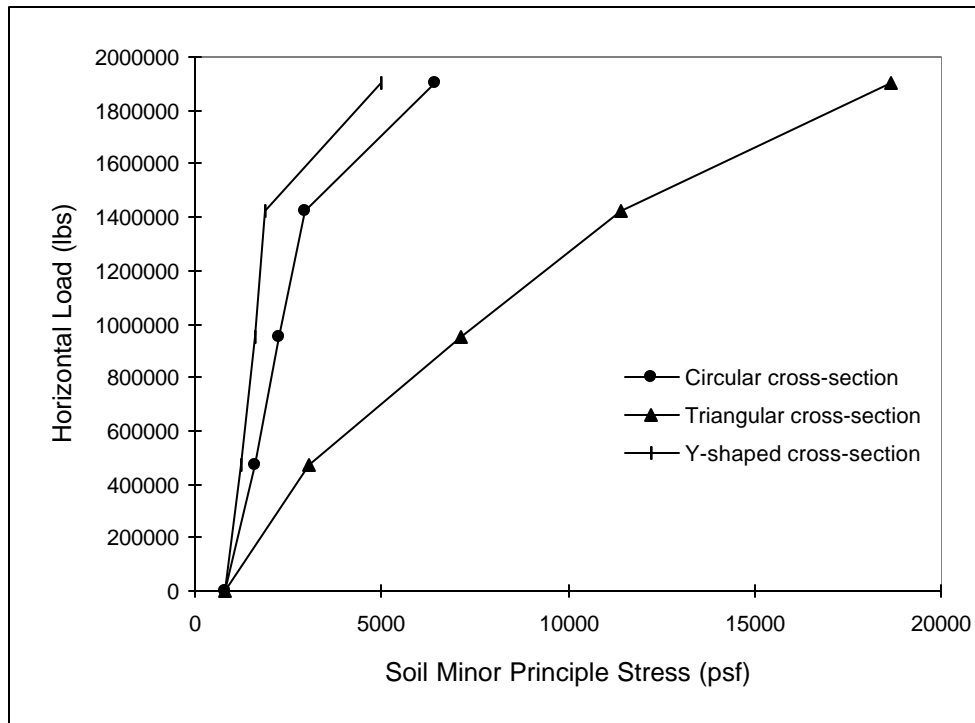
Figure 2. Minimum Soil Minor Principal Stress vs. Horizontal Load



occurred. To validate this reasoning, an additional plot was made for stresses at a given element. Figure 3 shows the relationship between the horizontal load and the soil minor principal stress of the element at the top of the advancing side of the pile. The inconsistent behavior of the Y-shaped cross-section as observed in Figure 2 is not evident in Figure 3. The yielding process of the soil in compression is clearly seen in the figure. As the horizontal load increased, the soil minor principal stresses increased linearly and then a subsequent yielding process occurred. As can be seen from the figure, the variations of the minimum soil minor principal stresses were similar for the circular and Y-shaped cross-sections. The rate of the soil stress increase with the increase in load for the triangular cross-section was much higher than the others. This is probably due to the stress concentration near the corners. The effect of the cross-section on the soil stress development became more significant at higher horizontal loads. The Y-shaped cross-section is the most effective in terms of the minimum soil minor principal stress.

As can be seen from Figure 2, when the horizontal load was less than 700,000 lbs, the Y-shaped cross-section experienced the smallest minimum soil minor principal stress, whereas the circular cross-section became the most effective for load magnitudes from 700,000 lbs to 1,700,000 lbs. Beyond the horizontal load of 1,700,000 lbs, the Y-shaped cross-section again became the most effective. The difference in stress magnitudes between the circular and Y-shaped cross-sections were, however, relatively small for loads less than 1,800,000 lbs, except near the load of 1,500,000 lbs where the difference exceeded 30%. The largest minimum soil minor principal stresses were always generated with the triangular cross-section.

Figure 3. Horizontal Load vs. Soil Minor Principal Stress of Element near the Top of the Advancing Side of the Pile



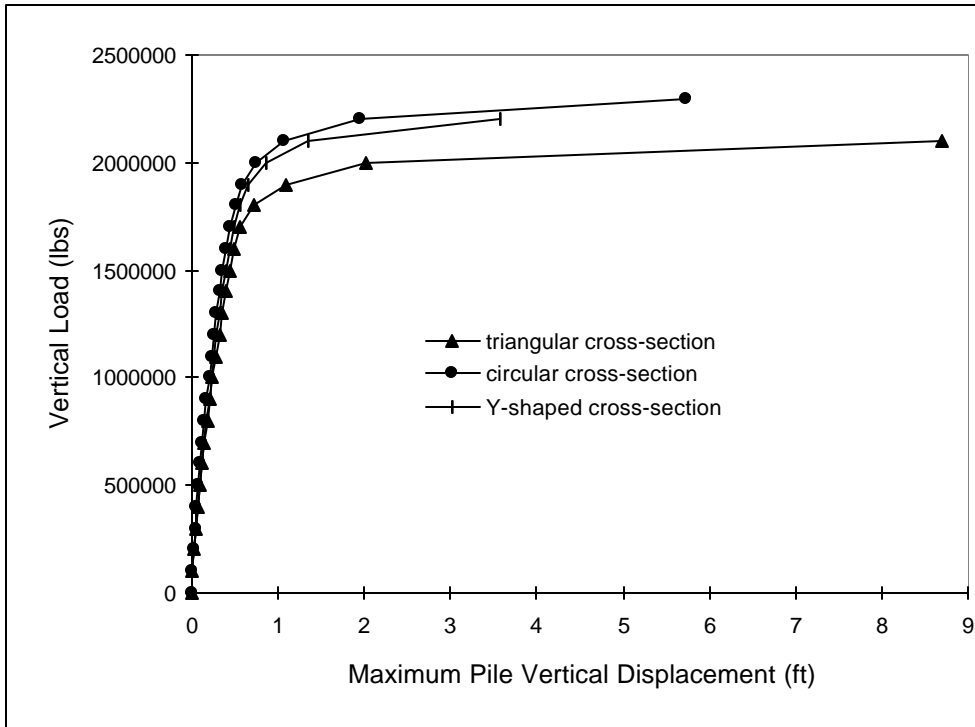
## Behaviors of Suction Piles under Vertical Tensile Loads

### 1) Maximum Pile Vertical Displacements

The maximum pile vertical displacement obtained from the finite element analysis was approximately the same as the maximum soil vertical displacement because the stiffness of the pile was assumed to be very large. With relatively large stiffness, the suction pile moved along the direction parallel to the loading direction with almost no relative deformation of the pile.

Figure 4 shows the distribution of the pile vertical displacements for the selected cross-sections at different vertical tensile loads applied at the center of the pile top. The relationship between the maximum vertical displacement and the vertical load shows the typical elasto-plastic behavior, i.e., a linear behavior at relatively low loads, followed by a nonlinear behavior due to the effect of the soil plasticity at relatively high loads. The smallest maximum vertical displacement at a given load was obtained with the circular cross-section. The largest maximum vertical displacement at a given load was generated with the triangular cross-section. The difference in displacements between the circular and Y-shaped cross-sections was insignificant before the yield occurred. However, the differences in displacements due to different cross-sections at the same vertical load increased with the increase in load. It is especially evident after the proportional limit reached. The proportional limit was observed to be approximately at the displacement of

Figure 4. Maximum Pile Vertical Displacement vs. Vertical Load



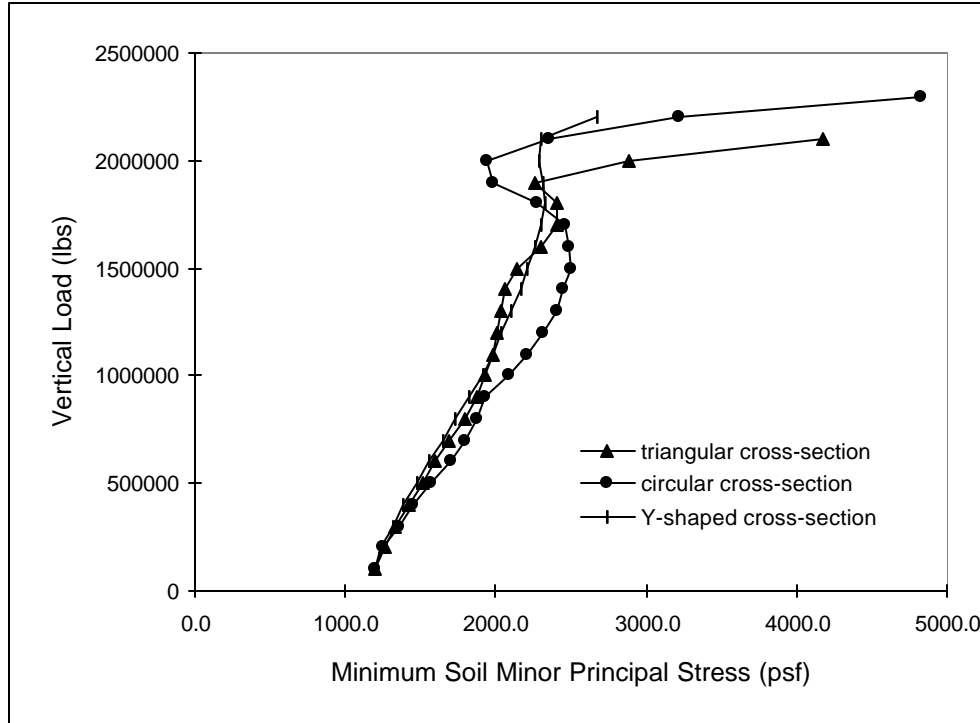
0.6 ft for all cross-sections.

## 2) Minimum Soil Minor Principal Stresses

As expected the minimum soil minor principal stresses due to various vertical loads were generated near the lower half around the pile. For triangular and Y-shaped cross-sections, the minimum soil minor principal stresses due to the vertical loads were generated near the corners within the lower half of the pile due to the stress concentration (Bang and Cho, 1998).

The relationship between the minimum soil minor principal stress and the vertical load is shown in Figure 5. Smallest minimum soil minor principal stresses due to vertical loads less than 1,700,000 lbs were generated with either the triangular (between 1,000,000 lbs and 1,700,000 lbs) or Y-shaped cross sections (between 100,000 lbs and 1,000,000 lbs). For vertical loads beyond 1,700,000 lbs, the minimum soil minor principal stresses for all cross-sections increased rapidly with no apparent pattern. The vertical load of 1,700,000 lbs corresponded approximately to the load associated with the elastic limit of the displacements (0.6 ft). The irregular variations of the stresses are resulted from reasons described previously.

Figure 5. Minimum Soil Minor Principal Stress vs. Vertical Load



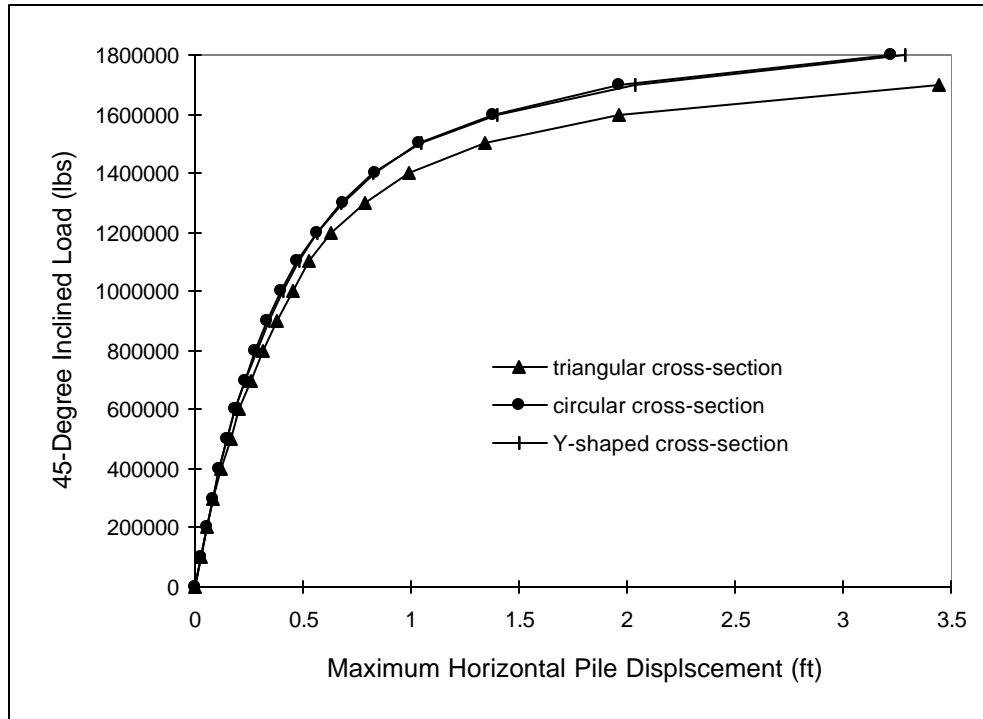
## Behaviors of Suction Piles under 45-Degree Inclined Tensile Loads

### 1) Maximum Pile Displacements

The largest horizontal displacement of the pile was always observed at the top of the pile, whereas the smallest horizontal displacement of the pile occurred at the bottom of the pile. As expected, the pile experienced translational as well as rotational movements (Bang and Cho, 1998).

Figures 6 shows the distributions of the pile horizontal displacements for the selected cross-sections at different inclined loads applied at the center of the pile top. Almost identical displacements were generated for the circular and Y-shaped cross-sections as was observed in the analysis for the horizontal loads. As the load increased, the displacements gradually approached the limiting values. The relationship is linear at lower loads, followed by a nonlinear behavior at higher loads due to the effect of the soil plasticity. The smallest vertical displacement at a given load was obtained with either the circular or the Y-shape cross-section, as was the case with horizontal loads. The differences in displacements with different cross-sections at a given load increased with the increase in load.

Figure 6. Maximum Horizontal Displacement vs. 45-Degree Inclined Load with the increase in load.



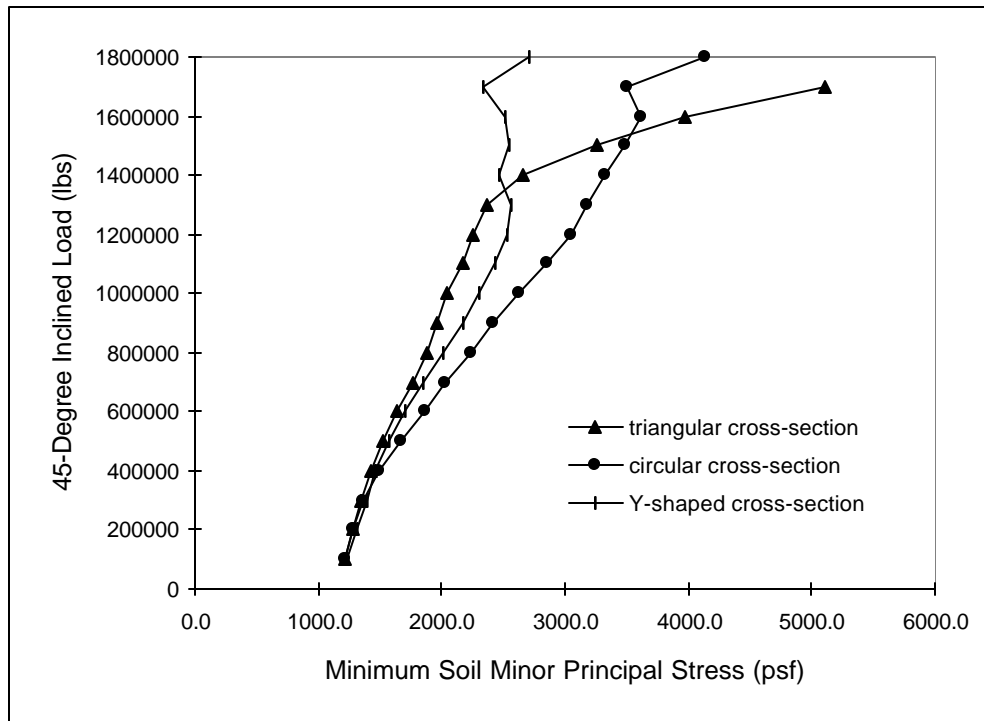
## 2) Minimum Soil Minor Principal Stresses

The relationship between the minimum soil minor principal stress and the 45-degree inclined load is shown in Figure 7. With the increase in load, the stresses showed irregular variations as seen in the other analyses. The smallest minimum soil minor principal stress for loads less than 1,300,000 lbs was observed with the triangular cross-section.

## CONCLUSIONS

From the results of the finite element analyses, it is evident that the effect of the soil plasticity is highly significant for large load magnitudes. General trends exist in terms of the overall responses of the pile under different applied loads. In general, the horizontal pile displacement due to the horizontal or 45-degree inclined loads applied at the center of the pile cap varies almost linearly under very low loads but becomes nonlinear under high loads for all cross-sections studied. The variation is apparently hyperbolic-shaped and gradually approaches to an ultimate value. The smallest pile displacement due to the horizontal or 45-degree inclined loads occurs with either the circular or the Y-shaped cross-section, depending upon the magnitude and direction of the applied load. On the other hand, the vertical pile displacement due to the vertical tensile load applied at the center of the pile cap exhibits a sudden yielding behavior at

Figure 7. Minimum Soil Minor Principal Stress vs. 45-Degree Inclined Load



displacement of approximately 0.6 ft for all cross-sections. The smallest displacement due to the vertical loads occurs always with the circular cross-section.

The minimum soil minor principal stresses due to the horizontal or 45-degree inclined loads applied at the center of the pile cap are dominated by the geostatic stress condition under low loads. However, as the geostatic stresses are gradually overcome, the minimum soil minor principal stresses due to the horizontal or 45-degree inclined loads develop at the bottom of the advancing side of the pile. The minimum soil minor principal stresses due to the vertical loads applied at the center of the pile cap are observed within the lower half of the pile. The smallest minimum soil minor principal stress depends on the direction and magnitude of the load. Under horizontal loads, the circular cross-section yielded the smallest stresses while the triangular cross-section generated the smallest stresses under inclined loads. When vertical loads are applied, the smallest stresses developed with the triangular and Y-shaped cross-section under smaller loads and higher loads, respectively.

#### 1) Pile Failure Load Based on Horizontal Displacement

Anderson et al. (1992) suggested from their model test results that the pile would fail against the lateral load when the pile experiences the rotation of 0.04 - 0.06 radians. For a 30 ft. long pile, the lateral displacement corresponding to this rotation is found to be 1.2 - 1.8 ft. Using the average value of 1.5 ft as the limiting lateral displacement of the pile, the horizontal and 45-degree inclined loads corresponding to the lateral

Table 1. Load Comparison at Horizontal Displacement of 1.5 ft

Horizontal Load (lbs)			45-Degree Inclined Load (lbs)		
Circle	Triangle	Y-shape	Circle	Triangle	Y-shape
1,471,000	1,408,000	1,484,000	1,620,000	1,525,000	1,616,000

displacement of 1.5 ft are summarized in Table 1, where the loads have been determined by a linear interpolation method.

As can be seen from Table 1, the Y-shaped cross-section allows the largest horizontal load of 1,484,000 lbs before the pile displacement reaches the limit value. While the circular cross-section exhibits the largest resistance of 1,620,000 lbs against the 45-degree inclined load, the difference in failure loads between the circular and the Y-shaped cross-section is very small (less than 0.8%). Table 1 also shows that the circular and Y-shaped cross-sections can resist approximately 5% and 6% more horizontal and 45-degree inclined loads than the triangular cross-section, respectively.

## 2) Pile Failure Load Based on Vertical Displacement

As described previously, the displacement pattern of the suction pile under vertical loads applied at the center of the pile cap shows an abrupt yield pattern. The yield displacement is approximately 0.6 ft for all cross-sections. The loads corresponding to the displacement of 0.6 ft are 1,910,000 lbs for the circular cross-section, 1,850,000 lbs for the Y-shaped cross-section, and 1,720,000 lbs for the triangular cross-section, respectively, indicating that the circular cross-section can provide the highest resistance against the vertical pull-out.

## ACKNOWLEDGEMENTS

The authors are grateful to the technical and financial supports provided by the US Office of Naval Research and the Naval Facilities Engineering Service Center. The work has been supported by the Department of the Navy, Office of Naval Research, grant number N00014-97-1-0887. The content of this paper does not necessarily reflect the position or the policy of the US Government.

## REFERENCES

- ABAQUS/Theory Manual (1997). Version 5.7, Ch. 4, Hibbitt, Karlsson & Sorensen Inc., USA.
- Anderson, K. H., R. Dyvik, and K. Schroder (1992). "Pullout Capacity Analysis of Suction Anchors for Tension Leg Platforms," Boss-92, 2, pp. 1311-1322.
- Bang S. and Y. Cho (1998). "Use of Suction Piles for Mooring of Mobile Offshore Bases – Performance Study." Task Completion Report, submitted to Naval Facilities Engineering Service Center.

- Drucker, D. C., and W. Prager (1952). "Soil Mechanics and Plastic Analysis or Limit Design," Quarterly of Applied Mathematics, Vol. 10, pp. 157-165.
- FEAMAP User's Manual (1986-1996), Version 4.5, Enterprise Software Products, Inc., Exton, PA.
- Lade, P. V. and K. L. Lee (1976). "Engineering Properties of Soils", UCLA Report No., UCLA-ENG-7652.
- Taylor, R. J. (1982). "Drag Embedded Anchor Tests in Sand and Mud", TN N-1635, Naval Civil Engineering Laboratory, Port Hueneme, CA.
- Ugural A. C. and S. K. Fenster (1995). *Advanced Strength and Applied Elasticity*, Third Edition, Ch.4, Prentice-Hall, Inc., NJ.